Journal of Applied Research and Technology

www.jart.ccadet.unam.mx
Journal of Applied Research and Technology 16 (2018) 346-356

Original

# Synthesis and characterization of gold nanoparticles on titanium dioxide for the catalytic photodegradation of 2,4-dichlorophenoxyacetic acid

Romero-Torres E.[a], Gutiérrez-Arzaluz M. [a,*], Mugica-Alvarez V.[a], González-Reyes L.[a], Torres-Rodríguez M. [a], Tzompantzi-Morales F.J.[b], Tzompantzi-Flores C.[b]

[a] *Departamento de Ciencias Básicas, Universidad Autónoma Metropolitana-Azcapotzalco. Av. San Pablo No.180, Colonia Reynosa Tamaulipas, 02200, Azcapotzalco, Ciudad de México, Mexico.*
[b] *Área de Ecocatálisis, Universidad Autónoma Metropolitana-Iztapalapa. Av. San Rafael Atlixco No. 186, Colonia Vicentina, 09340, Iztapalapa, Ciudad de México, Mexico.*

Received dd mm aaaa; accepted dd mm aaaa
Available online dd mm aaaa

**Abstract:** The photocatalytic degradation of 2,4-dichlorophenoxyacetic acid (2,4-D) using a $Au/TiO_2$ catalyst and ultraviolet (UV) light energy source (9 $mW/cm^2$) discussed. Gold nanoparticles were synthesized by controlled urea reduction and deposited on titanium dioxide ($TiO_2$) by the deposition-precipitation method. The average size of the nanoparticles was 6-8 nm. X-ray diffraction (XRD) characterization confirmed that $TiO_2$ was present in the anatase phase, whereas the presence and particle size of gold were determined by transmission electron microscopy (TEM). The results of the degradation showed that the activity of $TiO_2$ was improved when Au nanoparticles were present on the surface. The reactions were performed at atmospheric pressure and room temperature.

*Keywords:* Au nanoparticles, photodegradation, 2,4-dichlorophenoxyacetic acid

## 1. INTRODUCTION

Titanium dioxide ($TiO_2$) has been widely used for the photocatalytic degradation of organic compounds in water (Reddy, et al. 2016; Rammohan & Nadagouda, 2013). Recently, it was found that the dispersion of noble metal particles on the $TiO_2$ surface enhances its photocatalytic activity (Lee, Lintang, & Yuliati, 2017; Ravichandran, Selvam, Krishnakumar, & Swaminathan, 2009; Tang, et al., 2012). In addition, it was reported that the deposition of platinum and gold particles on titania can significantly inhibit electron-hole pair ($e^-/h^+$) recombination and provide a better response to wavelengths close to the visible region.

Noble metal nanoparticles (NPS), such as Au and Ag NPS, can generate localized surface plasmon resonance (LSPR) when they are irradiated with an energy source with a suitable wavelength (Bera, Lee, Rawal, & Lee, 2016). It is well known that the strength of the LSPR in NPS depends strongly on their properties, such as their size, shape and surface charge (Zhang, Chen, Liu, & Tsai, 2013; Wang, Dornom, Blackford, & Caruso, 2012).

* Corresponding author.
*E-mail address:* gam@correo.azc.uam.mx (Gutiérrez-Arzaluz M).

Peer Review under the responsibility of Universidad Nacional Autónoma de México.

Furthermore, noble metal nanoparticles, such as Au, Ag and Pt NPS, can strongly absorb visible light due to LSPR, which also depends on their size, shape and environment. Additionally, these NPS can act as both electron traps and active reaction sites (Wang, et al., 2012; Rayalu, et al., 2013).

Recently, it was reported that some photocatalytic reactions are strongly promoted by the LSPR effect of nanoparticle plasmons. Particularly, gold nanoparticles have been used as photocatalysts in the degradation of dyes (Mondal, Reyes, & Pal, 2017; Sobhana, Sarakha, Prevot, & Fardima, 2016), hydrogen generation (Rayalu, et al., 2013) and the degradation of phenol (Ayati, et al., 2014; Diak, et al., 2017). For these reasons, researchers have recently focused on supporting gold nanoparticles on titanium dioxide, which is a promising system for photocatalytic reactions and wastewater treatment.

Currently, due to their extensive use, some of the most common pollutants of wastewater from agricultural origins are pesticides and herbicides. Notably, 2,4-dichlorophenoxyacetic acid (2,4-D), the main herbicide used worldwide, has caused adverse impacts on ecosystems because of excessive exposure to it, and it is considered to be a possible endocrine disruptor and human carcinogen (Yu, et al., 2014). The degradation of 2,4-D has been widely studied by different techniques such as adsorption, biodegradation and ozonation (Lee, et al., 2017), but based on the reports of several researchers, its degradation via photocatalytic processes has been studied the most. Hu, et al. (2017) used $Cu_2(OH)PO_4$ as a microstructured photocatalyst and infrared light as a radiation source, whereas Lee, et al. (2017) used an $Fe_2O_3/TiO_2$ nanocomposite as a photocatalyst. Tang, et al. (2012) used a new photocatalyst consisting of Ag nanoparticles in reduced graphene oxide (RGO) on $TiO_2$ nanotubes. In another study, Liu, He, Liu, Liu, and Luo (2014) used CdTe nanoparticles with RGO on $TiO_2$ nanotubes. In contrast, Liu, et al. (2011) supported $CuInS_2$ nanoparticles on $TiO_2$ nanotubes; finally, Yu, et al. (2014) studied the role of $NO_2$ in the photodegradation of 2,4-D.

This work aims to improve the photoactivity of $TiO_2$ by surface modification of $TiO_2$ with gold the material with gold nanoparticles because this metal can inhibit the recombination of the excited electrons, enabling the holes to react more efficiently. This mechanism is the principal reason for the activity of this species in the oxidation of pollutants (Chen, Hua, Liu, Huang, & Jeng, 2009). To achieve the objective of this study, an $Au/TiO_2$ catalyst was synthesized by the deposition-precipitation method, which was reviewed by Zanella, Giorgio, Henry, and Louis (2002). This material was tested in the photodegradation of 2,4-dichlorophenoxyacetic acid.

## 2. EXPERIMENTAL

In the synthesis, commercial $TiO_2$ (Aldrich, 99% purity) was used as the support, the precursor salt for the Au nanoparticles was $HAuCl_4{*}3H_2O$ (Aldrich, 99% purity), and the reducing agent was urea (J.T. Baker, 99% purity). The $TiO_2$ support was dispersed in an aqueous solution of $HAuCl_4 \cdot 3H_2O$ to obtain gold loadings of 1 and 8 wt%. The solution was heated to 80°C, and after this temperature was reached, urea was added to a concentration of 0.42 M. The system was maintained under vigorous stirring for an aging period of 24 hours. After the aging period, the precipitated solid was washed with distilled water and dried at 80°C in a vacuum stove for 2 hours. Finally, the samples were subjected to thermal and reduction treatments; they were heated to 350°C at a rate of 2°C/min, maintained at this temperature for 3 hours under a hydrogen flux of 150 mL/min, and then cooled to room temperature under an $N_2$ atmosphere.

The synthesized catalyst was characterized by X-ray diffraction (XRD) using a Philips X'Pert diffractometer, and the morphology and metal content were determined by scanning electron microscopy and elemental analysis (SEM/EDS) using a Carl Zeiss Auriga microscope. The average size of the nanoparticles was determined by transmission electron microscopy (TEM) using a Jeol microscope, and the oxidation state was measured by XPS analysis using a MultiTech Specs instrument equipped with a dual Mg/Al X-ray source (XR50 model) and a PHOIBOS 150 hemispherical analyzer in the fixed analyzer transmission (FAT) mode.

The photocatalytic degradation of 2,4-D was performed in a photocatalytic reactor at atmospheric pressure and room temperature using a UV lamp ($9mW/cm^2$), 100 mg or 50 mg of the catalyst and 1 L of a 2,4-D solution (80 ppm). The concentration of 2,4-D was monitored using a Varian UV-Vis spectrometer. A control reaction with $TiO_2$ was also performed. The catalytic activity was determined by calculating the initial rates and conversion using the following equations:

$$X_{2,4D} = \frac{C^0_{2,4D} - C^t_{2,4D}}{C^t_{2,4D}} \bullet 100$$

$$-r_{2,4D} = C^0_{2,4D} \cdot \left[\frac{dX_{2,4D}}{dt}\right]_{t=0}$$

## 3. RESULTS AND DISCUSSION

### 3.1 CHARACTERIZATION

Figure 1 shows the diffraction patterns of the 1 and 8 wt% Au/$TiO_2$ samples and the $TiO_2$ support. In all three cases, the characteristic peaks of $TiO_2$, mainly the anatase phase, are observed as well-defined, intense peaks, especially for the sample with 1 wt% Au, which probably contains a minimum percentage of the rutile phase. This result is deduced from the support signal observed at 2θ=27.5° corresponding to the rutile phase. Overall, it is confirmed that Au incorporation onto the support does not modify its crystalline structure, and the anatase phase is preserved (DeSario, et al. 2013). For the 8 wt% Au/$TiO_2$ sample, diffraction peaks attributed to the Au structure (2θ=38.8°, 44.7°, 64.8°, 77.9°) (Wang, et al., 2012; Zielińska-Jurek, et al. 2011) are observed, but these peaks are not observed for the sample with 1 wt%, which suggests that its crystallite size is less than 10 nm. For the sample with 8wt% Au, the presence of Au diffraction peaks might be due to the high content of Au or the existence of large metal crystallites. The crystallite size of this sample is calculated to be 13.50 nm using the Scherrer equation with 2θ= 64.57° (Table 1). Using the peak at 2θ=25.32° corresponding to the (101) reflection plane of the anatase phase, the crystallite sizes of the titania supports were calculated for the three samples. Table 1 shows that the crystal size decreases as the Au content increases. This result might indicate an increase in the crystallinity of the anatase phase (Wang, et al., 2012).

Figure 2 shows the micrographs of the synthesized photocatalysts, which mainly reveal spherical, homogeneously sized $TiO_2$ crystals. In addition, bright spots corresponding to Au particles with nanometric dimensions are observed. Most of them have an average size of 4-6 nm, are spherically shaped, and are distributed homogeneously on the $TiO_2$ support. Both images show some clusters that are approximately 20 nm in size, which are probably responsible for the appearance of the diffraction peaks for Au in the XRD pattern of the sample with 8 wt% Au. The reduction conditions to which the materials are subjected do not promote the formation of larger particles. Therefore, it is assumed that the nanoparticles do not sinter, probably due to the good stabilization of the particles by the support.

The EDS profiles of the 1 and 8 wt% Au/$TiO_2$ powders, which are shown in Figure 3, reveal the presence of gold, oxygen and titanium. Based on these results, the Au contents of the synthesized powders were determined to be approximately 1.23 and 9.89 wt%, respectively, by a semiquantitative method. In both cases, the observed percentage is approximately 23% higher than the experimental percentage. This result might indicate that the synthesis method is adequate. The mapping of the 1 wt% Au/$TiO_2$ sample (see Figure 4) shows that gold is homogenously dispersed on the titania support.

Figure 5 shows the results of the TEM analysis. For the catalyst with 8 wt% Au, the average size of the nanoparticles ranges from 5 to 8 nm (Figure 5c). In contrast, for the sample with 1 wt% Au, the size is smaller than 5 nm (Figure 5a). The higher magnifications shown in Figures 5b and 5d confirm that in both materials, the gold nanoparticles are homogeneously distributed on the $TiO_2$ support after the sample is subjected to the reduction treatment.

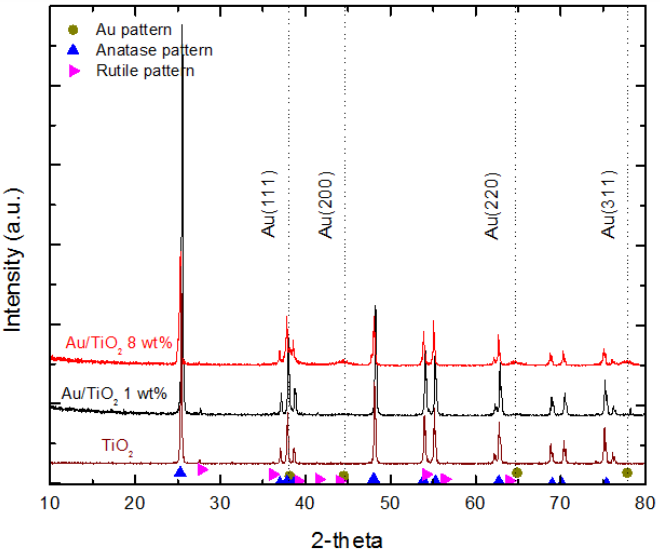


Fig. 1. XRD patterns of $TiO_2$ and 1 and 8 wt% Au/$TiO_2$

Detailed information about the chemical composition of and the valence states of the constituent elements in the 1 wt% Au/$TiO_2$ sample was determined by X-ray photoelectron spectroscopy (XPS). The spectrum in

Figure 6a shows the presence of Ti, O, Au and C on the sample surface. Figure 6b shows the spectrum of the Au *4f* core level for the sample. In this figure, two peaks, which are assigned to Au $4f_{7/2}$ and Au $4f_{5/2}$, are observed. In the literature, the binding energies for metallic Au are reported to be 82.8 eV and 86.6 eV (Grover, Singh, & Pal, 2014; Ying, Wang, Au, & Lai, 2010; Zielińska-Jurek, et al., 2011). In this study, the binding energies for Au/$TiO_2$ were determined to be Au $4f_{7/2}$=82.2 eV and Au $4f_{5/2}$=85.83 eV. These results might be due to the presence of a dominant $Au^{\delta-}$ species on the $TiO_2$ surface. The formation of this $Au^{\delta-}$ state could result from the interactions between $Au^0$ and the surface $Ti^{3+}$ centers, which would lead to the presence of titanium dioxide defects (Zielińska-Jurek, et al., 2011). Thus, it is deduced that gold is present in its reduced form on the titania surface. As shown in Figure 6c, Ti $2p_{3/2}$ and Ti $2p_{1/2}$ peaks with binding energies of 458.15 eV and 463.73 eV, respectively, are observed. The binding energy difference is $\Delta E_b$=5.58 eV, which is consistent with the reported value for $Ti^{4+}$ and thereby confirms the presence of $TiO_2$.

Finally, the spectrum in Figure 6d shows the high-resolution XPS analysis for the O *1s* core level. The representative peak is observed at 529.4 eV and is attributed to the Ti-O bond (Mohite et al., 2015). The C species observed in Figure 6e might be due to accidental carbon contamination, probably by the adsorption of carbon dioxide on the solid surface during sample preparation and the XPS analysis (Mohite et al., 2015). Hence, it can be concluded that the sample is composed of Ti, O and Au, based on the EDS and XRD results.

The spectrum in Figure 7 shows the UV-Vis analysis results for $TiO_2$ and the two samples impregnated with gold nanoparticles. For titania, an absorption band is observed at 340 nm (corresponding to 3.18 eV), which is a typical signal for anatase powder. As shown in Table 1, when $TiO_2$ strongly interacts with Au, the absorption band is slightly modified (DeSario, et al., 2013). Additionally, the sample with 1 wt% Au exhibits a surface plasmon resonance (SPR) at 550 nm. This feature, along with the low absorption, is characteristic of particles that are smaller than 5 nm. In contrast, the sample with 8 wt%

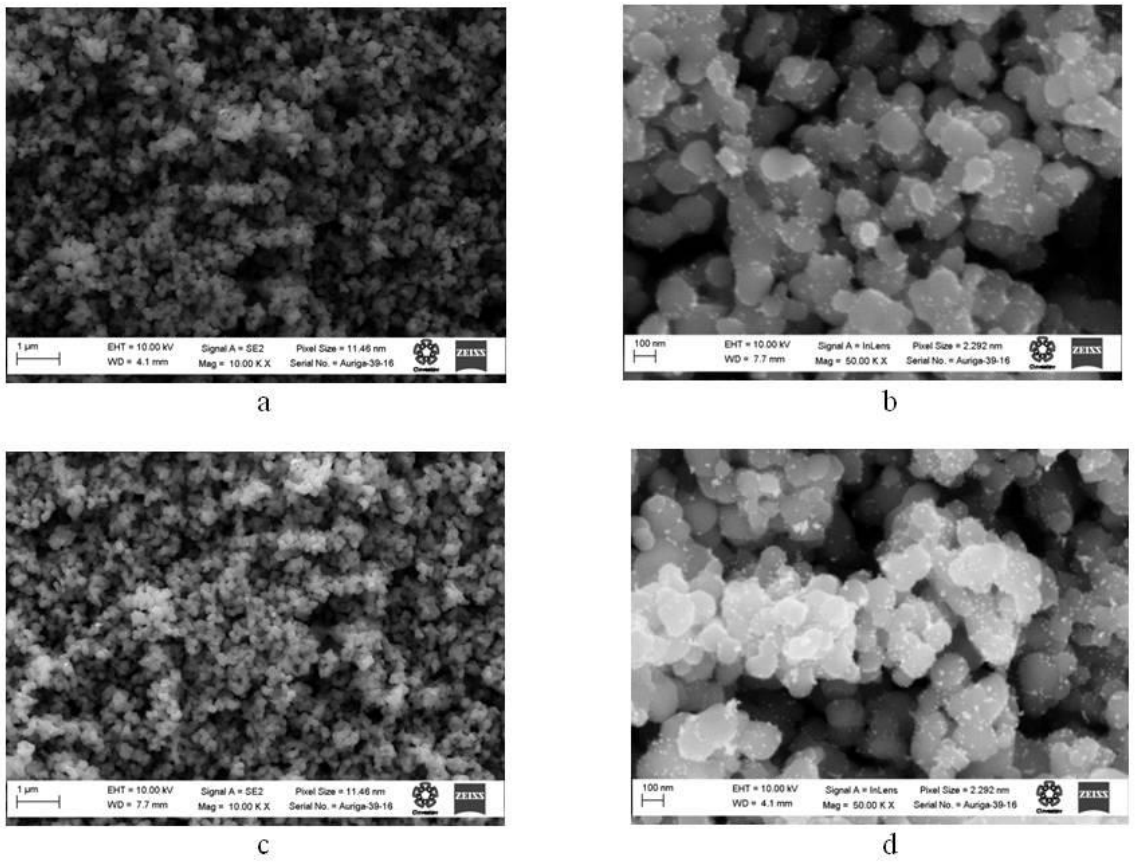


Fig. 2. SEM images of (a) 1 wt% Au/$TiO_2$ (1000kX), (b) 1 wt% Au/$TiO_2$ (50000kX), (c) 8 wt% Au/$TiO_2$ (1000kX) and d) 8 wt% Au/$TiO_2$ (50000kX).

Au exhibits higher absorption with two maxima at 458 and 587 nm. This result is probably due to the larger size of the gold nanoparticles (Zielińska-Jurek, et al., 2011). Also, the fact that, the surface plasmon band is very broad expanding, indicate a bimodal particle size distribution, mainly in the catalyst with 8 wt% Au, possible by the clusters observed by SEM for this sample.

The position and shape of the SPR band depends on several factors, such as the particle size, morphology and dielectric constant of the chemical environment (Liu, et al., 2014).

An intermediate absorption band is also observed at 400-450 nm for the Au samples, and it has a lower energy than the maximum of the $TiO_2$ band but a higher energy than the plasmon resonance. Furthermore, its absorbance increases as the Au content increases, which is consistent with results reported in the literature (DeSario, et al. 2013).

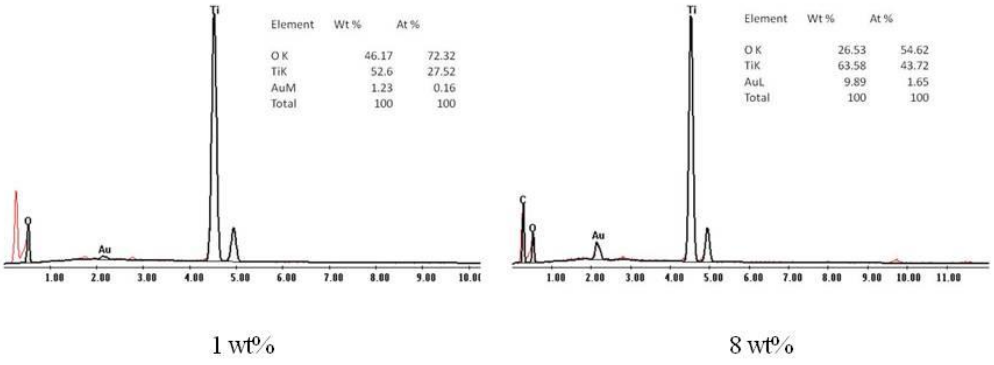


Fig. 3. EDS profiles of the 1 and 8 wt% Au/$TiO_2$ samples.

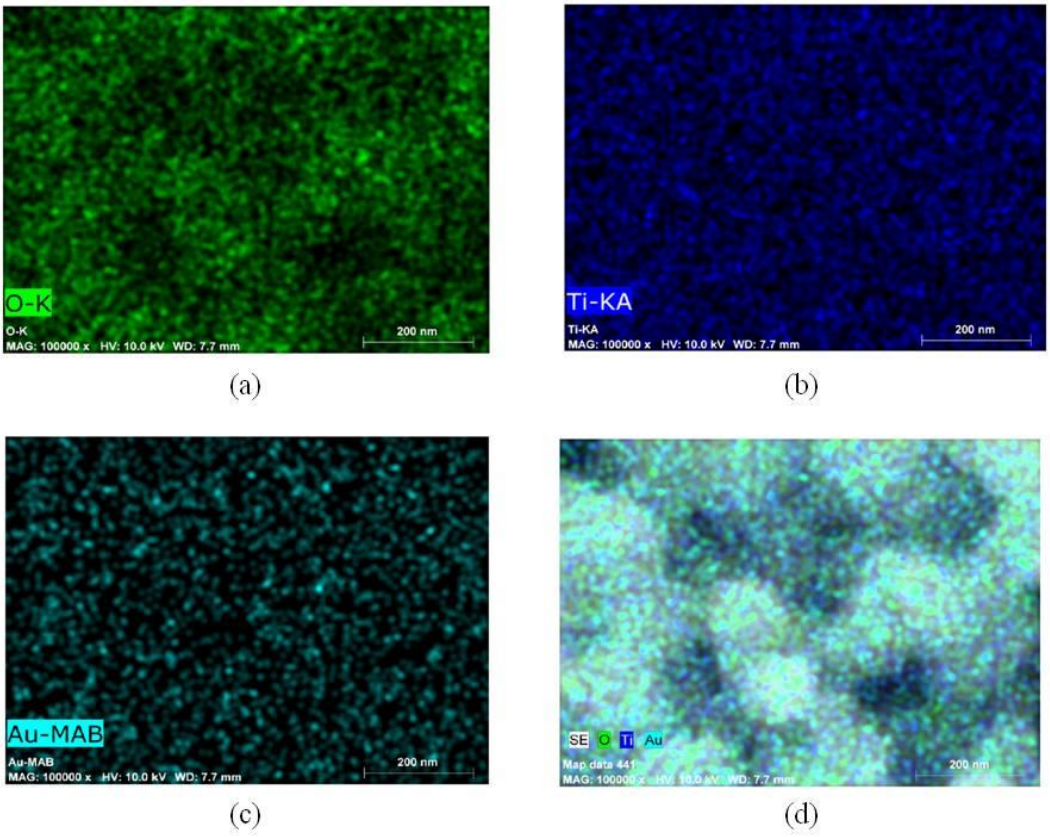


Fig. 4. SEM/EDS mapping of the 1 wt% Au/$TiO_2$ sample: a) O, b) Ti, c) Au, d) Au-Ti-O.

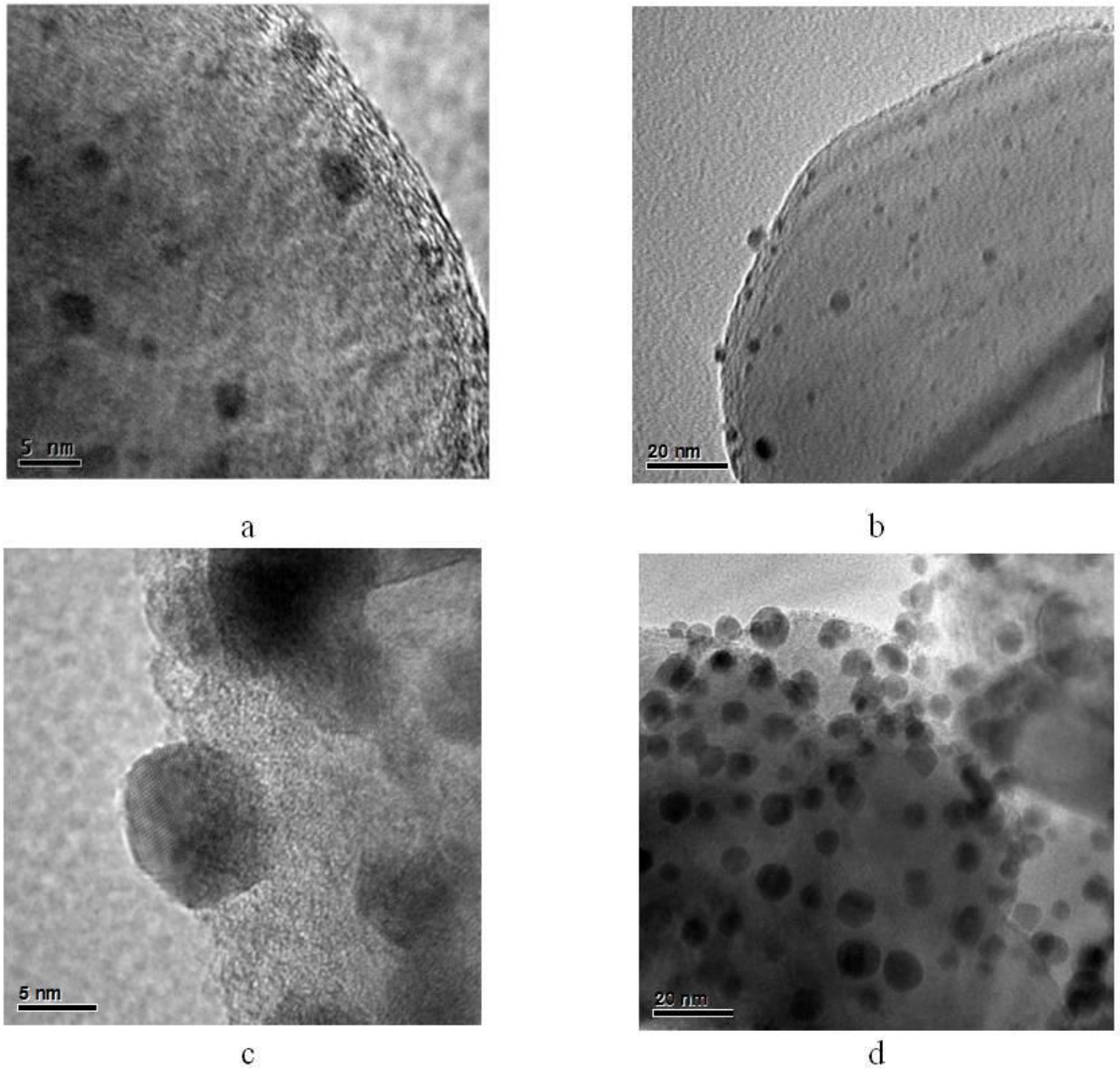


Fig. 5. TEM analysis: a) and b) 1 wt% Au/$TiO_2$, c) and d) 8 wt% Au/$TiO_2$.

Table 1. Effect of the Au content on the crystalline properties.

| Sample | Au Content (%) | $TiO_2$ Crystal Size[a] (nm) | Au Crystal Size[a] (nm) | Au Particle Size[b] (nm) | $TiO_2$ Abs. Maximum[c] (nm) | Au SPR Maximum[c] (nm) |
|---|---|---|---|---|---|---|
| **$TiO_2$** | | 105.3 | - | - | 332 | - |
| **Au/$TiO_2$** | 1 | 91.6 | n.i. | 4 ± 2 | 338 | 550 |
| **Au/$TiO_2$** | 8 | 72.0 | 13.51 | 8 ± 2 | 338 | 548 |

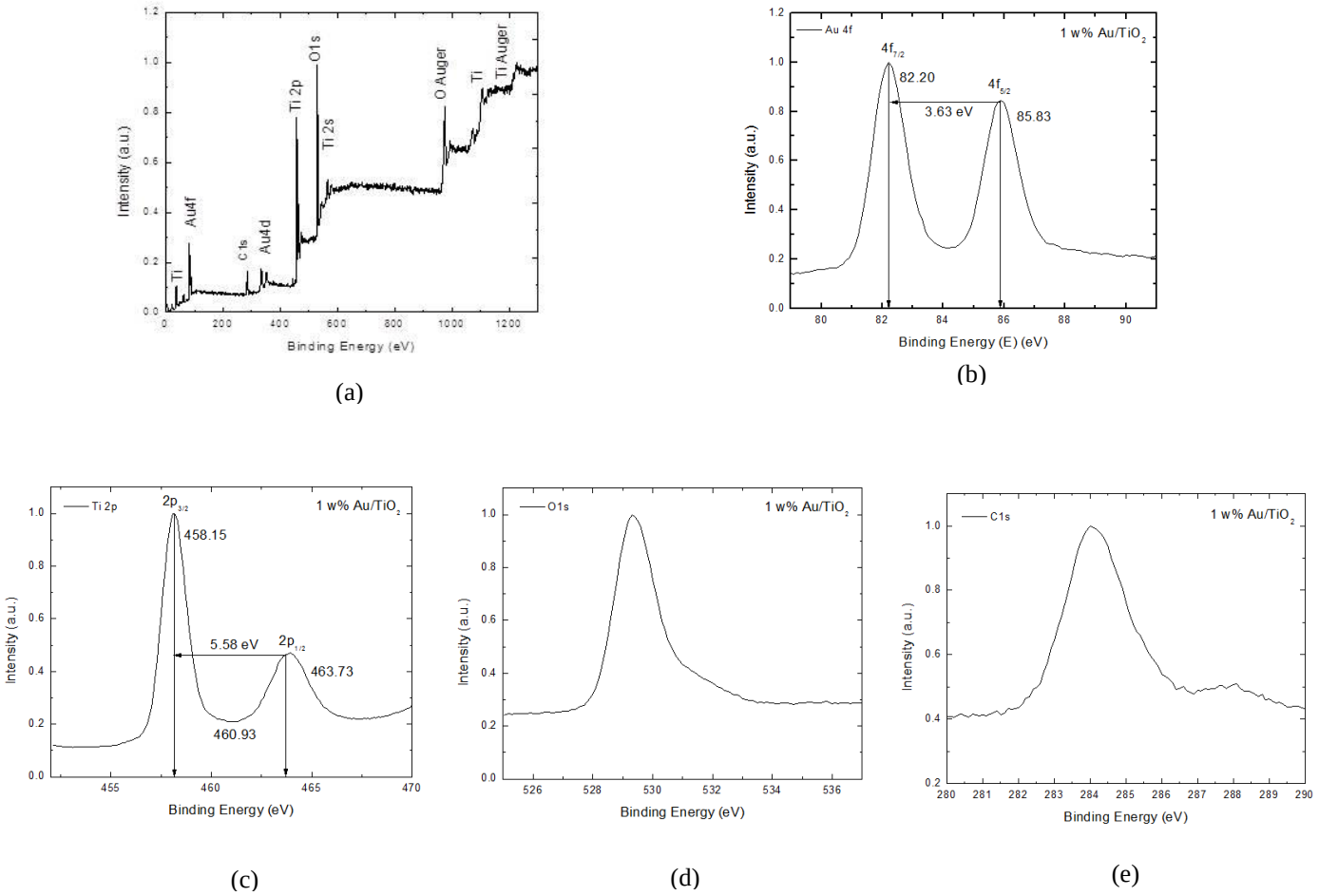


Fig. 6. a) Complete XPS spectrum of Au/$TiO_2$. b) Au *4f*, c) Ti *2p*, d) O *1s* and e) C *1s* spectra.

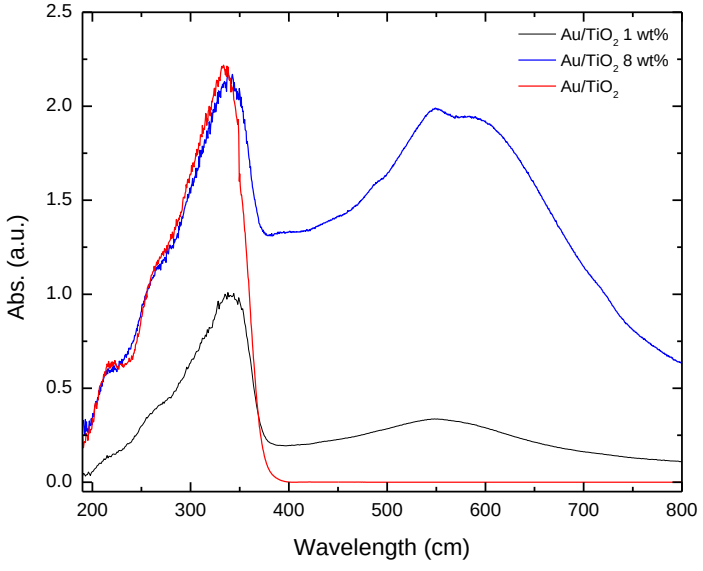


Fig. 7. UV-Vis spectra of the $TiO_2$ and 1 and 8 wt% Au/$TiO_2$ samples.

### 3.2 PHOTOCATALYSIS RESULTS

The photocatalytic activities of the materials with Au supported on $TiO_2$ for 2,4-D degradation were tested under UV light irradiation. Table 2 shows the results for the photocatalytic degradation of 2,4-D by the synthesized materials and for the photolysis reaction (without a catalyst). Under the tested experimental conditions (mass-volume ratio: 0.5 $g \cdot L^{-1}$, initial concentration: 80 ppm, reaction time: 6 hours), the photocatalytic activity is enhanced when the catalyst with 8 wt% Au is used; it is nearly 50% higher than the activity of photolysis. It should be noted that when a photocatalyst is used, the conversion after 1 hour of reaction is highly favorable, which is not the case in photolysis. It is well known that particles with the anatase structure exhibit higher photocatalytic activity (Wang, et al., 2012; Barakat, Hayes, & Ismat-Shah, 2005; Barakat, Schaeffer, Hayes, & Ismat-Shah, 2005). The crystalline nature of the anatase structure is mainly responsible for the photocatalytic activity of the nanoparticles. In addition, as shown by the XRD results listed in Table 1, the particle size of $TiO_2$ decreases as the Au content increases, which could be an important factor contributing to the activity improvement because the photocatalyst then has a higher surface area where the catalytic reactions can occur. In this way, the photoreactivity of the samples is enhanced by not only a higher gold content but also a higher surface area. It is also important to highlight that the particle size of Au is not a determining factor for the pollutant photodegradation in this work; the elimination percentage is slightly lower for the sample with 1 wt% Au, which has a smaller particle diameter than the sample with 8 wt% Au. It should also be noted that the initial reaction rate is one order of magnitude higher for the sample with 8 wt% Au. This behavior, i.e., the high photocatalytic activities of large Au particles, has already been observed by other researchers in the photodegradation of dyes, such as methylene blue (Wang, et al., 2012) and phenolic compounds (Murdoch, et al., 2011). Table 3 shows the results for the analysis of the effects of the initial solution concentration on the photode-gradation of 2,4-D. For each of the three photocatalysts, two different initial concentrations were studied using a mass-volume ratio of 0.5 $g \cdot L^{-1}$ and a reaction time of only 240 min. Clearly, the results show that at the lower initial pollutant concentration, the conversion is higher for all three tested catalysts. This phenomenon was also observed in heterogeneous catalytic systems in which the reaction occurred at the solid interphase in the biphasic or triphasic system (Barakat, Schaeffer, et al., 2005) and in other photocatalytic studies (Wang, et al., 2012). Therefore, it can be concluded that the photocatalytic activity is usually high when the pollutant concentration is low. The effect of the initial solution concentration observed in the tests with the catalyst with 8 wt% Au is not significant compared to those observed in the tests with $TiO_2$ and the catalyst with 1 wt% Au. Compared to the results for the catalyst with 8 wt% Au, the conversion for the catalyst with 1 wt% Au is slightly higher at 40 ppm, and its initial reaction rate at 40 ppm is twice that at 80 ppm. Specifically, the conversion is 5% higher at 40 ppm than at 80 ppm. The initial reaction rate is higher for the solution with the higher initial concentration. Seck, et al. (2012) also observed this behavior for 2,4-D degradation by $TiO_2$ nanoparticles synthesized by several different methods. Additionally, some authors have suggested that the high reaction rate must be due to a high pollutant concentration over a large specific surface area. In this work, it can be indirectly attributed to this effect, because the sample has a smaller $TiO_2$ crystal size, resulting in a larger specific surface area of the catalytic support on which the photocatalytic reaction can occur. Finally, Table 4 shows the results for the effect of the catalyst mass on the elimination of 2,4-D obtained with the sample with 1 wt% Au. The mass-volume ratios studied were 0.25, 0.5 and 1.0 $g \cdot L^{-1}$; the initial concentration was 80 ppm; and the reaction time was 6 hours. The results show that the most efficient pollutant photodegradation is achieved at the lowest mass-volume ratio. Several authors reported that the pollutant photodegradation rate is influenced by the amount of active sites on and the absorption capacity of the catalyst (Doon & Chang, 1998; Shankar, Anandan, Venkatachalam, Arabindoo, & Murugesan 2006; Trillas, Peral, & Domènech, 1995). Therefore, it can be assumed that when the catalyst loading is increased, the formation rate of the electron/hole pair increases, thereby enhancing the pollutant photodecomposition. Nevertheless, Barakat, et al., (2005) found that large amounts of the photocatalyst in the reaction suspension obstructed the UV light irradiation, which led to a reduction in the photodegradation rate. In this work, a high conversion and high initial rates are achieved in the pollutant elimination when the mass-volume ratio of the photocatalyst in the suspension is the lowest.

Table 2. Effect of the catalyst on the photocatalytic degradation of 2,4-D.

| Sample | Au Content (%) | Concentration (80 ppm) | | |
|---|---|---|---|---|
| | | $-r_{2,4\text{-}D,0}$[a] ($mol \cdot L^{-1} \cdot min^{-1}$) | $-r_{2,4\text{-}D,0}$[a] ($mg \cdot L^{-1} \cdot min^{-1}$) | $X_{2,4\text{-}D}$[b] (%) |
| Photolysis | - | $0.905 \cdot 10^{-6}$ | $0.2 \cdot 10^{-2}$ | 50.46 |
| $TiO_2$ | - | $2.352 \cdot 10^{-5}$ | $5.2 \cdot 10^{-2}$ | 82.16 |
| $Au/TiO_2$ | 1 | $4.433 \cdot 10^{-5}$ | $9.8 \cdot 10^{-2}$ | 93.30 |
| $Au/TiO_2$ | 8 | $13.39 \cdot 10^{-5}$ | $29.6 \cdot 10^{-2}$ | 98.15 |

[a] Determined at the initial time. [b] After 360 min of reaction.

Table 3. Effect of the initial concentration on the degradation of 2,4-D.

| Sample | Au content (%) | Concentration (40 ppm) | | Concentration (80 ppm) | |
|---|---|---|---|---|---|
| | | $-r_{2,4\text{-}D,0}$[a] ($mg \cdot L^{-1} \cdot min^{-1}$) | $X_{2,4\text{-}D}$[b] (%) | $-r_{2,4\text{-}D,0}$[a] ($mg \cdot L^{-1} \cdot min^{-1}$) | $X_{2,4\text{-}D}$[b] (%) |
| **$TiO_2$** | - | $13.1 \cdot 10^{-2}$ | 75.11 | $5.2 \cdot 10^{-2}$ | 40.28 |
| **$Au/TiO_2$** | 1 | $17.8 \cdot 10^{-2}$ | 86.30 | $9.8 \cdot 10^{-2}$ | 37.90 |
| **$Au/TiO_2$** | 8 | $20.7 \cdot 10^{-2}$ | 85.00 | $29.6 \cdot 10^{-2}$ | 80.42 |

Table 4. Effect of the catalyst mass (1 wt% $Au/TiO_2$) on the photocatalytic degradation of 2,4-D.

| Mass of Catalyst (g) | Mass/Volume Ratio ($g \cdot L^{-1}$) | Concentration (80 ppm) | | |
|---|---|---|---|---|
| | | $-r_{2,4\text{-}D,0}$[a] ($mol \cdot L^{-1} \cdot min^{-1}$) | $-r_{2,4\text{-}D,0}$[a] ($mg \cdot L^{-1} \cdot min^{-1}$) | $X_{2,4\text{-}D}$[b] (%) |
| 50 | 0.25 | $12.90 \cdot 10^{-5}$ | $28.7 \cdot 10^{-2}$ | 98.14 |
| 100 | 0.50 | $4.43 \cdot 10^{-5}$ | $9.8 \cdot 10^{-2}$ | 93.30 |
| 200 | 1.00 | $3.53 \cdot 10^{-5}$ | $7.8 \cdot 10^{-2}$ | 71.51 |

[a] Determined at the initial time. [b] After 360 min of reaction.

## 4. CONCLUSIONS

The XRD and SEM/EDS result, showed it is possible to obtain Au nanoparticles (NPS) supported on commercial $TiO_2$ by the deposition-precipitation method and according to the TEM results, nanoparticles of 5-8 nm and of less than 5 nm are obtained on the catalysts with 8 and 1 wt% Au, respectively. The photocatalytic results show to the initial photocatalytic activity results, the elimination of 2,4-D increases when Au is present. The catalyst with 1wt% Au has a slightly larger conversion than $TiO_2$. Therefore, it is concluded that the presence of gold, and not its particle size, promotes the elimination of 2,4-D in this study. The results clearly show that the conversion is higher at a lower initial pollutant concentration. Furthermore, a high conversion and high initial rates of reaction are obtained for the pollutant elimination at the lowest mass-volume ratio of the photocatalyst in the suspension studied.

The highest photocatalytic activity is observed for the sample with 8 wt% Au. In addition, the pollutant elimination is clearly more efficient when the initial concentration of 2,4-D and the mass of catalyst in the suspension are lower. Finally, it is concluded that the presence of nanoparticles increases the initial reaction rate relative to that observed for the $TiO_2$ control. The improvement in the photocatalytic activity is attributed to the crystallinity and nanometric size of the material and to the reduction in the band gap.

## ACKNOWLEDGEMENTS

Mirella Gutiérrez gratefully acknowledges CONACyT's (Mexico) Basic Science project for its financial support of this research. Additionally, GM, MV, TM and TF gratefully thank the SNI for the distinction of their membership and the stipend.

## CONFLICT OF INTEREST

The authors have no conflicts of interest to declare.

## REFERENCES


Ayati, A., Ahmadpour, A., Bamoharram, F. F., Tanhaei, B., Mänttäri, M., & Sillanpää, M. (2014). A review on catalytic applications of Au/TiO2 nanoparticles in the removal of water pollutant. Chemosphere, 107, 163-174. https://doi.org/10.1016/j.chemosphere.2014.01.040

Barakat, M. A., Hayes, G., & Shah, S. I. (2005). Effect of cobalt doping on the phase transformation of TiO2 nanoparticles. Journal of nanoscience and nanotechnology, 5(5), 759-765. http://www.physics.udel.edu/~ismat/2005p3.pdf

Barakat, M. A., Schaeffer, H., Hayes, G., & Ismat-Shah, S. (2005). Photocatalytic degradation of 2-chlorophenol by Co-doped TiO2 nanoparticles. Applied Catalysis B: Environmental, 57(1), 23-30. https://doi.org/10.1016/j.apcatb.2004.10.001

Bera, S., Lee, J. E., Rawal, S. B., & Lee, W. I. (2016). Size-dependent plasmonic effects of Au and Au@ SiO2 nanoparticles in photocatalytic CO2 conversion reaction of Pt/TiO2. Applied Catalysis B: Environmental, 199, 55-63. https://doi.org/10.1016/j.apcatb.2016.06.025

Chen, Z. Y., Hu, Y., Liu, T. C., Huang, C. L., & Jeng, T. S. (2009). Mesoporous TiO2 thin films embedded with Au nanoparticles for the enhancement of the photocatalytic properties. Thin Solid Films, 517(17), 4998-5000. https://doi.org/10.1016/j.tsf.2009.03.189

DeSario, P. A., Pietron, J. J., DeVantier, D. E., Brintlinger, T. H., Stroud, R. M., & Rolison, D. R. (2013). Plasmonic enhancement of visible-light water splitting with Au–TiO 2 composite aerogels. Nanoscale, 5(17), 8073-8083.

Diak, M., Klein, M., Klimczuk, T., Lisowski, W., Remita, H., Zaleska-Medynska, A., & Grabowska, E. (2017). Photoactivity of decahedral TiO2 loaded with bimetallic nanoparticles: degradation pathway of phenol-1-13C and hydroxyl radical formation. Applied Catalysis B: Environmental, 200, 56-71. https://doi.org/10.1016/j.apcatb.2016.06.067

Doong, R. A., & Chang, W. H. (1998). Photodegradation of parathion in aqueous titanium dioxide and zero valent iron solutions in the presence of hydrogen peroxide. Journal of Photochemistry and Photobiology A: Chemistry, 116(3), 221-228.https://doi.org/10.1016/S10106030(98)00292-5

Grover, I. S., Singh, S., & Pal, B. (2014). Influence of thermal treatment and Au-loading on the growth of versatile crystal phase composition and photocatalytic activity of sodium titanate nanotubes. RSC Advances, 4(93), 51342-51348. DOI: 10.1039/C4RA06605G

Hu, C., Li, P., Zhang, W., Che, Y., Sun, Y., Chi, F., ... & Lv, Y. (2017). Effect of Cupric Salts (Cu (NO3) 2, CuSO4, Cu (CH3COO) 2) on Cu2 (OH) PO4 Morphology for Photocatalytic Degradation of 2,4-dichlorophenol under Near-infrared light irradiation.*Materials Research*, *20*(2), 407-412.http://dx.doi.org/10.1590/1980-5373-mr-20160561

Lee, S. C., Lintang, H. O., & Yuliati, L. (2017). High photocatalytic activity of Fe2O3/TiO2 nanocomposites prepared by photodeposition for degradation of 2, 4-dichlorophenoxyacetic acid. *Beilstein journal of nanotechnology*, *8*, 915. doi: 10.3762/bjnano.8.93. eCollection 2017.

Liu, M., He, L., Liu, X., Liu, C., & Luo, S. (2014). Reduced graphene oxide and CdTe nanoparticles co-decorated TiO2 nanotube array as a visible light photocatalyst. *Journal of materials science*, *49*(5), 2263-2269. DOI 10.1007/s10853-013-7922-4

Liu, R., Liu, Y., Liu, C., Luo, S., Teng, Y., Yang, L., ... & Cai, Q. (2011). Enhanced photoelectrocatalytic degradation of 2, 4-dichlorophenoxyacetic acid by CuInS2 nanoparticles deposition onto TiO2 nanotube arrays. *Journal of Alloys and Compounds*, *509*(5), 2434-2440. https://doi.org/10.1016/j.jallcom.2010.11.040

Mohite, V. S., Mahadik, M. A., Kumbhar, S. S., Hunge, Y. M., Kim, J. H., Moholkar, A. V., ... & Bhosale, C. H. (2015). Photoelectrocatalytic degradation of benzoic acid using Au doped TiO2 thin films. *Journal of Photochemistry and Photobiology B: Biology*, *142*, 204-211. https://doi.org/10.1016/j.jphotobiol.2014.12.004

Mondal, S., Reyes, M. E. D. A., & Pal, U. (2017). Plasmon induced enhanced photocatalytic activity of gold loaded hydroxyapatite nanoparticles for methylene blue degradation under visible light. *RSC Advances*, *7*(14), 8633-8645. DOI: 10.1039/C6RA28640B

Murdoch, M. G. I. N., Waterhouse, G. I. N., Nadeem, M. A., Metson, J. B., Keane, M. A., Howe, R. F., ... & Idriss, H. (2011). The effect of gold loading and particle size on photocatalytic hydrogen production from ethanol over Au/TiO 2 nanoparticles. *Nature Chemistry*, *3*(6), 489. doi:10.1038/nchem.1048

Rammohan, G., & N Nadagouda, M. (2013). Green photocatalysis for degradation of organic contaminants: a review. *Current Organic Chemistry*, *17*(20), 2338-2348. http://dx.doi.org/10.2174/13852728113179990039

Ravichandran, L., Selvam, K., Krishnakumar, B., & Swaminathan, M. (2009). Photovalorisation of pentafluorobenzoic acid with platinum doped TiO2. *Journal of hazardous materials*, *167*(1-3), 763-769. https://doi.org/10.1016/j.jhazmat.2009.01.048

Rayalu, S. S., Jose, D., Joshi, M. V., Mangrulkar, P. A., Shrestha, K., & Klabunde, K. (2013). Photocatalytic water splitting on Au/TiO2 nanocomposites synthesized through various routes: enhancement in photocatalytic activity due to SPR effect. *Applied Catalysis B: Environmental*, *142*, 684-693. https://doi.org/10.1016/j.apcatb.2013.05.057

Reddy, P. A. K., Reddy, P. V. L., Kwon, E., Kim, K. H., Akter, T., & Kalagara, S. (2016). Recent advances in photocatalytic treatment of pollutants in aqueous media. *Environment international*, *91*, 94-103. https://doi.org/10.1016/j.envint.2016.02.012

Seck, E. I., Doña-Rodríguez, J. M., Fernández-Rodríguez, C., González-Díaz, O. M., Araña, J., & Pérez-Peña, J. (2012). Photocatalytic removal of 2, 4-dichlorophenoxyacetic acid by using sol–gel synthesized nanocrystalline and commercial TiO2: Operational parameters optimization and toxicity studies. *Applied Catalysis B: Environmental*, *125*, 28-34. DOI: 10.1016/j.apcatb.2012.05.028

Shankar, M. V., Anandan, S., Venkatachalam, N., Arabindoo, B., & Murugesan, V. (2006). Fine route for an efficient removal of 2, 4-dichlorophenoxyacetic acid (2, 4-D) by zeolite-supported TiO2. *Chemosphere*, *63*(6), 1014-1021. https://doi.org/10.1016/j.chemosphere.2005.08.041

Sobhana, L., Sarakha, M., Prevot, V., & Fardim, P. (2016). Layered double hydroxides decorated with Au-Pd nanoparticles to photodegradate Orange II from water. *Applied Clay Science*, *134*, 120-127. https://doi.org/10.1016/j.clay.2016.06.019

Tang, Y., Luo, S., Teng, Y., Liu, C., Xu, X., Zhang, X., & Chen, L. (2012). Efficient removal of herbicide 2, 4-dichlorophenoxyacetic acid from water using Ag/reduced graphene oxide co-decorated $TiO_2$ nanotube arrays. *Journal of hazardous materials*, *241*, 323-330. https://doi.org/10.1016/j.jhazmat.2012.09.050

Trillas, M., Peral, J., & Domènech, X. (1995). Redox photodegradation of 2, 4-dichlorophenoxyacetic acid over TiO2. *Applied Catalysis B: Environmental*, *5*(4), 377-387. https://doi.org/10.1016/0926-3373(94)00058-1

Wang, P., Huang, B., Dai, Y., & Whangbo, M. H. (2012). Plasmonic photocatalysts: harvesting visible light with noble metal nanoparticles. *Physical Chemistry Chemical Physics*, *14*(28), 9813-9825. DOI: 10.1039/c2cp40823f

Wang, X., Dornom, T., Blackford, M., & Caruso, R. A. (2012). Solvothermal synthesis and photocatalytic application of porous Au/TiO 2 nanocomposites. *Journal of Materials Chemistry*, *22*(23),11701-11710. DOI: 10.1039/C2JM31759A

Yinga, F., Wang, S., Au, C. T., & Lai, S. Y. (2010). Effect of the oxidation state of gold on the complete oxidation of isobutane on Au/ CeO $_2$ catalysts. *Gold Bulletin*, *43*(4), 241-251.

Yu, C., Wang, H., Liu, X., Quan, X., Chen, S., Zhang, J., & Zhang, P. (2014). Photodegradation of 2, 4-D induced by NO2− in aqueous solutions: The role of NO2. *Journal of Environmental Sciences*, *26*(7), 1383-1387. https://doi.org/10.1016/j.jes.2014.05.002

Zanella, R., Giorgio, S., Henry, C. R., & Louis, C. (2002). Alternative methods for the preparation of gold nanoparticles supported on $TiO_2$. *The Journal of Physical Chemistry B*, *106*(31), 7634-7642. DOI: 10.1021/jp0144810

Zhang, X., Chen, Y. L., Liu, R. S., & Tsai, D. P. (2013). Plasmonic photocatalysis. *Reports on Progress in Physics*, *76*(4), 046401.

Zielińska-Jurek, A., Kowalska, E., Sobczak, J. W., Lisowski, W., Ohtani, B., & Zaleska, A. (2011). Preparation and characterization of monometallic (Au) and bimetallic (Ag/Au) modified-titania photocatalysts activated by visible light. *Applied Catalysis B: Environmental*, *101*(3-4), 504-514. https://doi.org/10.1016/j.apcatb.2010.10.022